



TID Effects of High-Z Material Spot Shields on FPGA Using MPTB Data

*S.H. Crain, J.E. Mazur, and M.D. Looper
The Aerospace Corporation, El Segundo, California*



Prepared for Marshall Space Flight Center
under H-Order 32489D
and sponsored by
The Space Environments and Effects Program
managed at the Marshall Space Flight Center

The NASA STI Program Office...in Profile

Since its founding, NASA has been dedicated to the advancement of aeronautics and space science. The NASA Scientific and Technical Information (STI) Program Office plays a key part in helping NASA maintain this important role.

The NASA STI Program Office is operated by Langley Research Center, the lead center for NASA's scientific and technical information. The NASA STI Program Office provides access to the NASA STI Database, the largest collection of aeronautical and space science STI in the world. The Program Office is also NASA's institutional mechanism for disseminating the results of its research and development activities. These results are published by NASA in the NASA STI Report Series, which includes the following report types:

- **TECHNICAL PUBLICATION.** Reports of completed research or a major significant phase of research that present the results of NASA programs and include extensive data or theoretical analysis. Includes compilations of significant scientific and technical data and information deemed to be of continuing reference value. NASA's counterpart of peer-reviewed formal professional papers but has less stringent limitations on manuscript length and extent of graphic presentations.
- **TECHNICAL MEMORANDUM.** Scientific and technical findings that are preliminary or of specialized interest, e.g., quick release reports, working papers, and bibliographies that contain minimal annotation. Does not contain extensive analysis.
- **CONTRACTOR REPORT.** Scientific and technical findings by NASA-sponsored contractors and grantees.

- **CONFERENCE PUBLICATION.** Collected papers from scientific and technical conferences, symposia, seminars, or other meetings sponsored or cosponsored by NASA.
- **SPECIAL PUBLICATION.** Scientific, technical, or historical information from NASA programs, projects, and mission, often concerned with subjects having substantial public interest.
- **TECHNICAL TRANSLATION.**
English-language translations of foreign scientific and technical material pertinent to NASA's mission.

Specialized services that complement the STI Program Office's diverse offerings include creating custom thesauri, building customized databases, organizing and publishing research results...even providing videos.

For more information about the NASA STI Program Office, see the following:

- Access the NASA STI Program Home Page at <http://www.sti.nasa.gov>
- E-mail your question via the Internet to help@sti.nasa.gov
- Fax your question to the NASA Access Help Desk at (301) 621-0134
- Telephone the NASA Access Help Desk at (301) 621-0390
- Write to:
NASA Access Help Desk
NASA Center for AeroSpace Information
7121 Standard Drive
Hanover, MD 21076-1320
(301)621-0390



TID Effects of High-Z Material Spot Shields on FPGA Using MPTB Data

*S.H. Crain, J.E. Mazur, and M.D. Looper
The Aerospace Corporation, El Segundo, California*

Prepared for Marshall Space Flight Center
under H-Order 32489D
and sponsored by
The Space Environments and Effects Program
managed at the Marshall Space Flight Center

National Aeronautics and
Space Administration

Marshall Space Flight Center • MSFC, Alabama 35812

Acknowledgments

This effort was accomplished with resources provided by NASA's Living With a Star (LWS) Space Environment Testbeds (SET) Program.



Available from:

NASA Center for AeroSpace Information
7121 Standard Drive
Hanover, MD 21076-1320
(301) 621-0390

National Technical Information Service
5285 Port Royal Road
Springfield, VA 22161
(703) 487-4650

TABLE OF CONTENTS

1. INTRODUCTION	1
1.1 Background and Overview	1
1.2 MPTB FPGA Experiment Board	1
1.3 Icc Degradation	2
1.4 Summary	4
2. ENVIRONMENT DATA SOURCE	5
2.1 Environment Measurements for Input to Radiation Transport Calculations.....	5
3. DATA PROCESSING	7
3.1 Code Packages.....	7
3.2 Simulation Geometries.....	7
4. DATA ANALYSIS	8
4.1 Dose Calculation and Limitations of Simulated Physics	8
4.2 Low Energy Photons	11
5. SUMMARY AND CONCLUSIONS.....	12
6. REFERENCES	13

LIST OF FIGURES

1.	Pictures of the space side (left and vehicle side (right) of the FPGA board. The stiffener was attached using the holes at the sides of the board. It was a 25.4 mm (1") wide bar running parallel to the connector, across the shielded devices	1
2.	A sketch of the layers of shielding over two of the A1460As. The cross-section shows the materials make-up and thickness relative to position in space	2
3.	The I_{cc} , normalized for all DUTs, is shown relative to a series of geomagnetic storms. The devices with the CuW shields (3 and 4) are experiencing greater increases in I_{cc} than the unshielded devices (1, 2, and 5)	3
4.	Again, the normalized supply current for each device is shown relative to geomagnetic storms. The large proton event in July of 2000 does not have the same effect as the electron storms in August and September	3
5.	Compares the 3 integral spectra we used in detailed monte-carlo radiation transport calculations described below. The AE-8 MAX curve describes the average HEO environment calculated with the AE-8 model	6
6.	The dose rate is shown for 3 spectra: the AE8 MAX model, the HEO worst-case as calculated by Fennell, etal, and the very hard spectrum for the August 1998 geomagnetic storm	8
7.	The integral electron and photon spectra reaching the die for 5 MeV incident electrons in both devices without the spot shield (a) and with (b)	9
8.	The integral photon spectra for all devices are very similar for 5 MeV electrons	9
9.	At 6 MeV incident electrons, the integral photon spectra for the shielded devices begins to exceed that for the unshielded at low energies	10
10.	The low energy enhancement for the photon spectra reaching the die of the shielded parts is more pronounced for the 8 MeV incident electrons	10
11.	With 10 MeV incident electrons, the photon spectra for the shielded devices shows an enhancement for all energies up to 5 MeV reaching the die	11

1. INTRODUCTION

1.1 Background and Overview

In an experiment on the Microelectronics and Photonics Test Bed (MPTB) that was testing field programmable gate arrays, spot-shields were used to extend the life of some of the devices being tested. It was expected that the unshielded parts would fail from total ionizing dose (TID) and yet the opposite has happened. The data shows that the devices failing from the TID effect are the ones with the spot-shields attached.

We had previously established that this effect could be correlated to geomagnetic storms.[1] In this study, we attempted to determine the mechanism by which the environment is interacting with the high-Z material to enhance the TID in these field programmable gate arrays (FPGAs).

1.2 MPTB FPGA Experiment Board

The FPGA experiment board on MPTB tests 5 identically programmed A1460A FPGAs from Actel for single event upset (SEU). The current consumption (I_{cc}) of each device is monitored as a measure of total ionizing dose accumulated over the time the experiment is active. This is considered to be the determining parameter for TID tolerance in these FPGA devices. The basic mechanisms for the radiation-induced leakage currents have been well established (e.g. ref[2]). I_{cc} is a measure of this leakage current.

The devices under test (DUTs) on this experiment board are located on either side of the experiment board (see Figure 1), powered by either 5V or 3.3V, and either covered by an additional gold-plated copper tungsten (CuW) shield and aluminum stiffener or not. The configuration for each DUT is shown in Table 1.

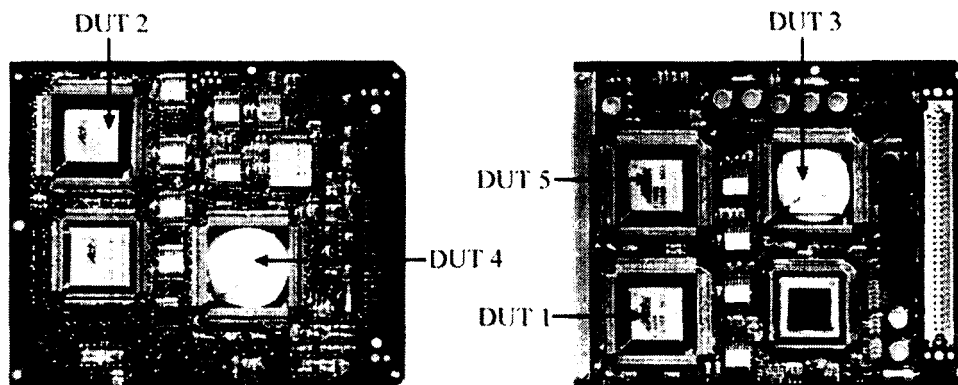


Figure 1. Pictures of the space side (left) and vehicle side (right) of the FPGA board. The stiffener was attached using the holes at the sides of the board. It was a 25.4 mm (1") wide bar running parallel to the connector, across the shielded devices.

TABLE I – DUT CONFIGURATION

DUT Number	IC Supply Voltage	Location	Shielding in addition to the lid
DUT 1	3.3 V	Vehicle-side	No shielding or stiffener
DUT 2	3.3 V	Space-side	No shielding or stiffener
DUT 3	3.3 V	Vehicle-side	Stiffener and CuW Shield
DUT 4	5 V	Space-side	Stiffener and CuW Shield
DUT 5	5 V	Vehicle-side	No shielding or stiffener

A1460A-CQ196B Lot date code 961

The entire experiment board is covered by an aluminum lid that is 1.66 mm thick. The spot-shields that were added to two of the devices are 5.08 mm (0.2") copper/tungsten with a small amount of nickel and gold plating. The density is about 18g/cm^3 . The aluminum stiffener across the board is 5.59 mm (220 mil) thick and 25.4 mm (1") wide and spans across the two shielded devices and the controller chip (an A1280A FPGA also from Actel, spot shielded with tantalum and located on the vehicle-side of the board). The two DUTs with spot shielding are back-to-back on the board. Figure 2 is a sketch of the cross-section of these two DUTs.

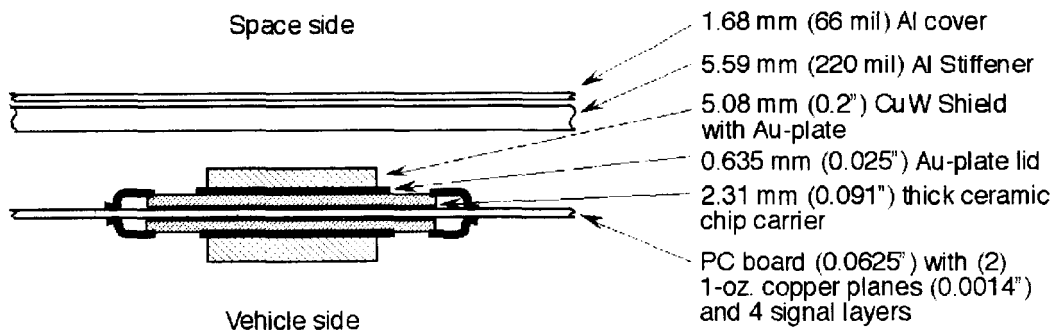


Figure 2. A sketch of the layers of shielding over two of the A1460As. The cross-section shows the materials' make-up and thickness relative to position in space.

1.3 Icc Degradation

The I_{cc} (supply current) for all the DUTs first increased noticeably with the onset of a series of geomagnetic storms in August of 1998. DUT 4, the CuW shielded part powered with 5V, had the largest current increase as shown in Figure 3. By the 4th storm in the series, DUT3, the other CuW shielded device, which is powered with 3.3V, also began to experience a greater increase in I_{cc} .

The delay in the total dose response of DUT3 can be explained by the lower supply voltage (V_{cc}). A lower V_{cc} will reduce the radiation-induced holes trapped in the field oxide that would cause the leakage channel leading to the increase in I_{cc} (e.g. ref[2]). That is, the total dose threshold is higher for devices powered with a lower supply voltage.

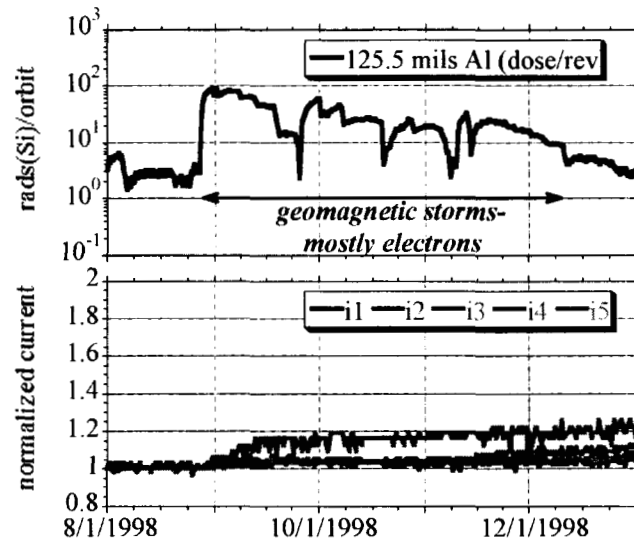


Figure 3. The I_{cc} , normalized for all DUTs, is shown relative to a series of geomagnetic storms. The devices with the CuW shields (3 and 4) are experiencing greater increases in I_{cc} than the unshielded devices (1, 2, and 5).

Since the storms in August 1998 were immediately preceded by a large proton event, it is not clear from this time period if the electrons alone were affecting the shielded devices. However, the data taken in the summer of 2000 shows that the large proton event known as the Bastille Day event (onset was July 14th) had little effect but the geomagnetic storms a month later were better correlated with the current consumption (see Fig. 4).

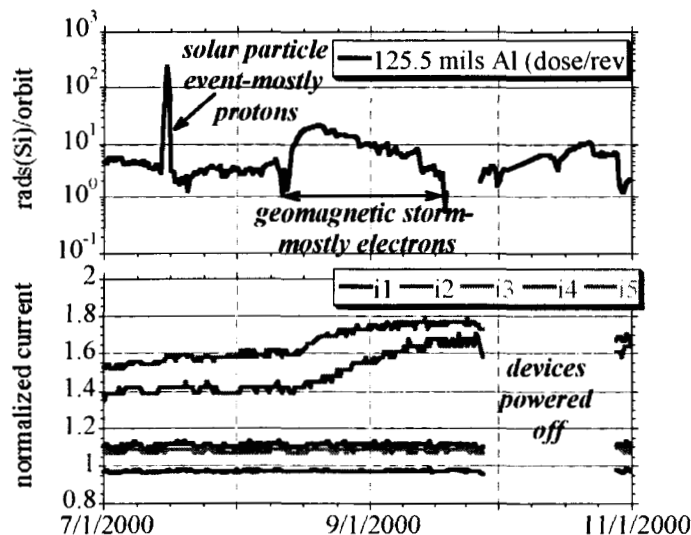


Figure 4. Again, the normalized supply current for each device is shown relative to geomagnetic storms. The large proton event in July of 2000 does not have the same effect as the electron storms in August and September.

1.4 Summary

We undertook a course of simulations using actual environment measurements in space during the periods of interest in order to better understand the data. We found that indeed the spectrum of energies for the series of storms in the fall of 1998 was much harder than predicted by models such as AE-8 MAX. The transport code calculations show a resultant increase in the photon spectra reaching the die for these higher electron energies. And finally, the codes have limitations in correctly simulating the physics of the interactions of radiation with matter at the device level.

2. ENVIRONMENT DATA SOURCE

2.1 Environment Measurements for Input to Radiation Transport Calculations

During geomagnetic storms such as the ones shown in Figures 3 & 4, the actual electron spectra are much different both in absolute intensity as well as spectral shape from those predicted by models such as the AE-8 MAX model. Such models are representative of average activity over several solar cycles. Thus, to more accurately model the dose in the various materials in Figure 2, we sought to develop representative event spectra based on measurements during the events in question. We focused on the energetic, trapped electrons since the most significant response of the DUTs occurred during enhancements of these particles. We also considered the 2000 July 14 solar energetic particle event in the analysis for comparison since there was not a corresponding response in the Icc of the DUTs.

It is difficult to accurately measure the energy spectra of energetic (>1 MeV) electrons because of scattering in detector material and scattering from materials adjacent to the detector (e.g. ref [3]). Keeping in mind these experimental difficulties, we began a comparison of the measurements available from the NASA/Polar satellite as well as inferred electron count rates from the dosimeters on board the same HEO (highly elliptical orbit) vehicle on which MPTB rode. There are uncertainties in absolute calibration in individual instruments. It was also the case that the 1998 August geomagnetic storm was intense enough to saturate the electron detector on the Polar satellite. In principle, the dose rate from the dosimeters (measured in rads/orbit) should be free from saturation since they measure the total energy deposit regardless of how frequently the electrons trigger their counting threshold. The total energy deposit is then proportional to the number of electrons above the energy threshold.

In this study of the intense radiation environment in 1998 August, we therefore used the electron spectrum measured with dosimeters on the HEO vehicle. We also considered a “worst-case” HEO electron spectrum developed for an internal charging specification (Fennell et al. 1999, ref[4]). Figure 5 compares these three spectra. Both the Fennell et al. spectrum and the 1998 August spectrum were much higher in intensity than the AE-8 model.

For the analysis of the response to the 2000 July 14 proton event, we used a total fluence spectrum measured in interplanetary space on several NASA science satellites during the interval from 10:00Z on 14 July to 10:00Z on 18 July. The differential spectrum was fitted to a curve with formula

$$j(E) = 1.43e9 * E^{(-1.14)} * \exp(-E/31.72),$$

with j the fluence in protons per (cm² sr MeV) and E the proton energy in MeV. This was multiplied by 4π steradians to get an omnidirectional differential fluence in protons per (cm² MeV), then added up to get an omnidirectional integral fluence in protons per cm².

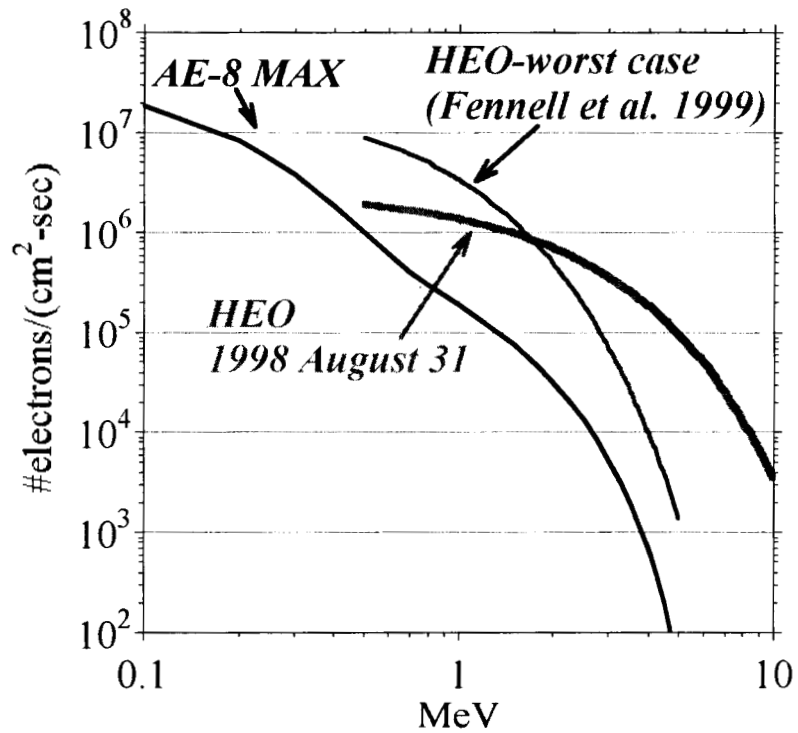


Figure 5. Compares the 3 integral spectra we used in detailed monte-carlo radiation transport calculations described below. The AE-8 MAX curve describes the average HEO environment calculated with the AE-8 model.

3. DATA PROCESSING

3.1 Code Packages

The primary radiation-transport code used in this work has been EGSnrc, which is an improvement (mostly due to the efforts of the National Research Council of Canada, whence the “nrc” in the name) of the EGS4 electromagnetic Monte Carlo code package. In the first part of this study we used EGS4, then, in order to improve the physics, performed those simulations again using a new installation of EGSnrc; we then carried out all further work using EGSnrc. The main improvements in the code concentrated on its simulation of low-energy radiation transport (between 1 keV and 1 MeV), which is the range of interest to us here. We also attempted to cross-check our results using GEANT4, a general-purpose nuclear and electromagnetic radiation-transport code [i.e., one that simulates the behavior of protons, neutrons, and other heavy particles, as well as electrons, positrons, and photons]. In the available time we did not succeed in getting this code package working correctly for the low-energy electrons and photons of interest.

3.2 Simulation Geometries

First, we calculated dose in the electronic parts under shielding appropriate to different parts of the experiment box; the simulation used was accurate in three dimensions, with materials and geometry as in the actual installation (e.g., a stepped chip carrier made of silica). The next set of simulations used the same realistic geometry, but we explored dependence of our dose results on our geometric assumptions by varying the thickness of the Cu-W shields and gold plating. In the third quarter, we examined the individual particles (electrons, photons, and positrons) reaching the die through the Cu-W shield; to do this we reverted to a simpler geometry, with an infinite slab of Cu-W illuminated on one side by electrons. In the final quarter, we studied individual particles reaching each die in the realistic geometry, again with varying shield thicknesses but (constant) real dimensions for the board and electronic parts.

4. DATA ANALYSIS

4.1 Dose Calculation and Limitations of Simulated Physics

Early in our study we determined that even using the actual environment spectra in the transport code, we could not calculate a higher dose in the shielded parts than that in the unshielded ones. Figure 6 plots the dose rates for the different spectra into the devices.

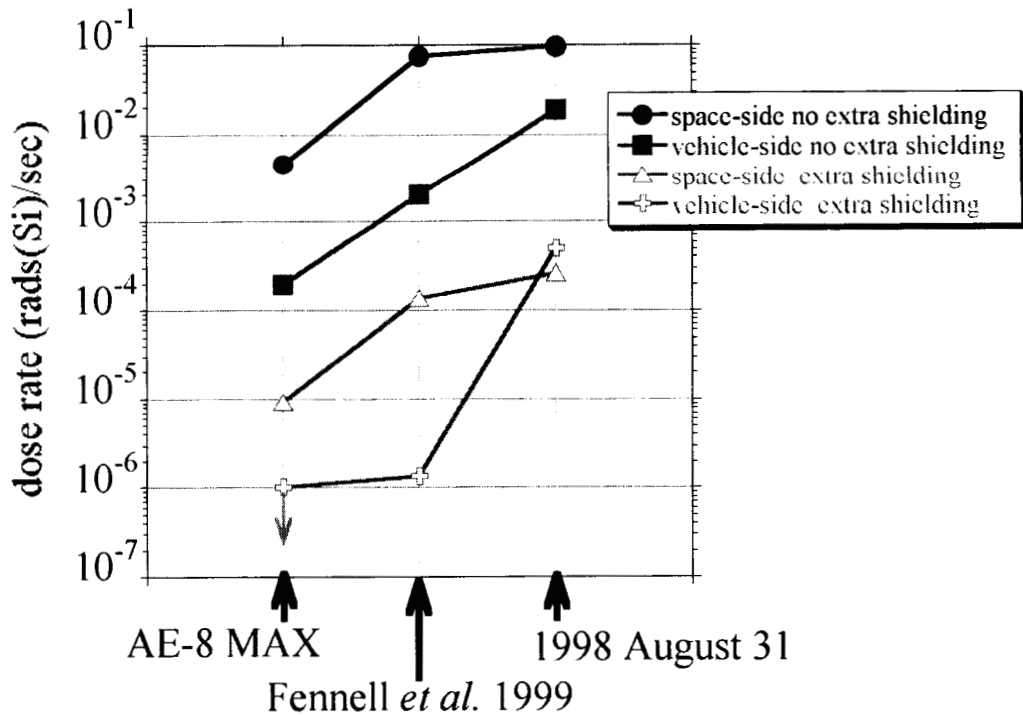


Figure 6. The dose rate is shown for 3 spectra: the AE8 MAX model, the HEO worst-case as calculated by Fennell, *et al.*, and the very hard spectrum for the August 1998 geomagnetic storm.

In the dose calculations, we did not find any case where increasing the shielding caused more bulk dose in the silicon; this is why, midway through the project, we shifted the focus of our simulations to the individual particles reaching the parts. While we found that more shielding generally reduced the number of electrons reaching each die, we also found that, for the highest-energy incident electrons, thicker shielding resulted in more photons of energies up to about 1 MeV reaching the electronic parts. Figure 7 shows the electron and photon spectra for the devices with and without the spot shielding for 5 MeV incident electrons. The shielding significantly reduces the electrons reaching the die. However, for incident electrons with energies of about 5 MeV and higher, the lower-energy photons begin to increase. The trend is demonstrated in Figs. 8-11, the photon spectra for 5, 6, 8, and 10 MeV respectively.

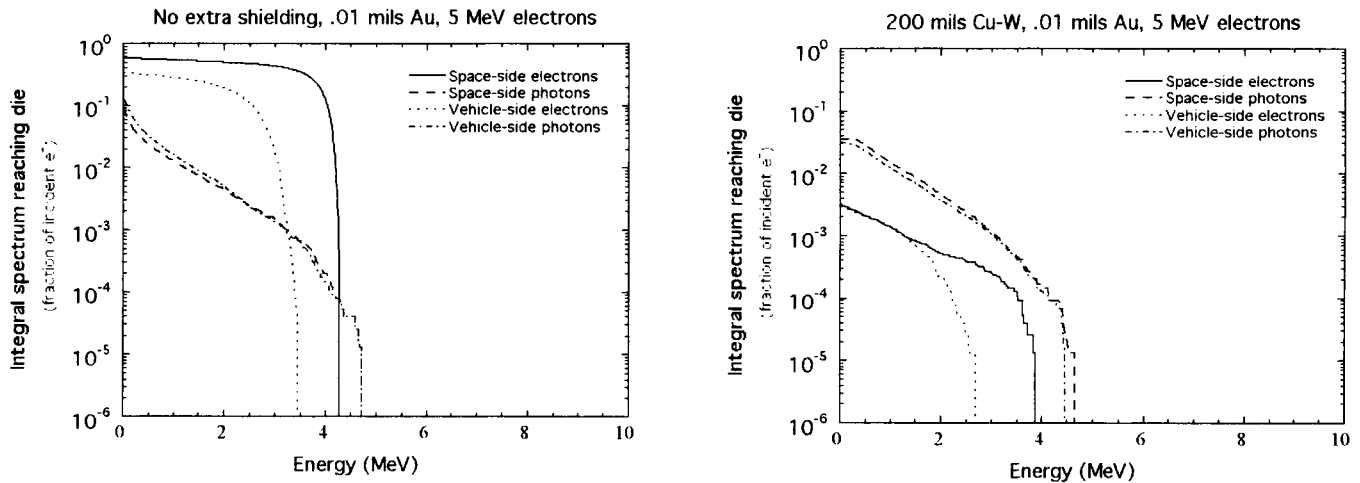


Figure 7. The integral electron and photon spectra reaching the die for 5 MeV incident electrons in both devices without the spot shield (a) and with (b).

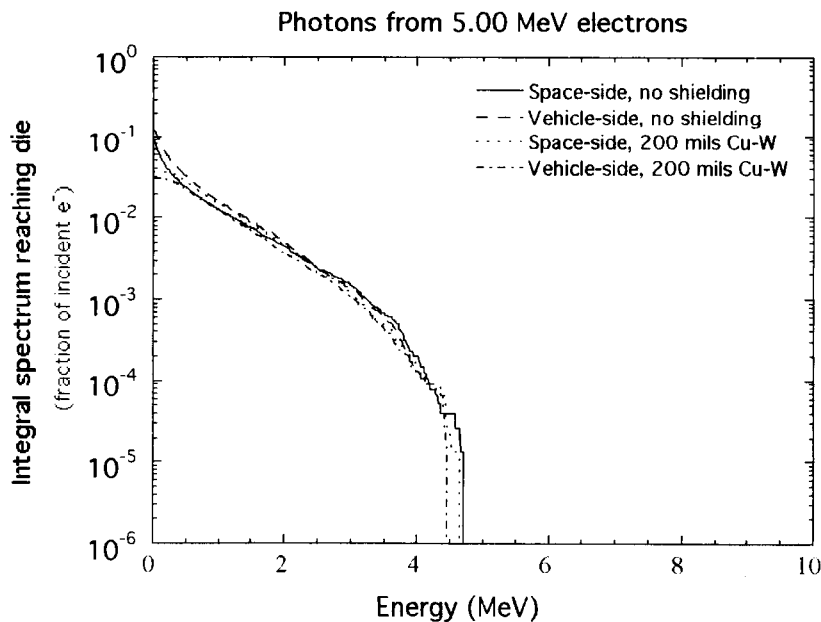


Figure 8. The integral photon spectra for all devices are very similar for 5 MeV electrons.

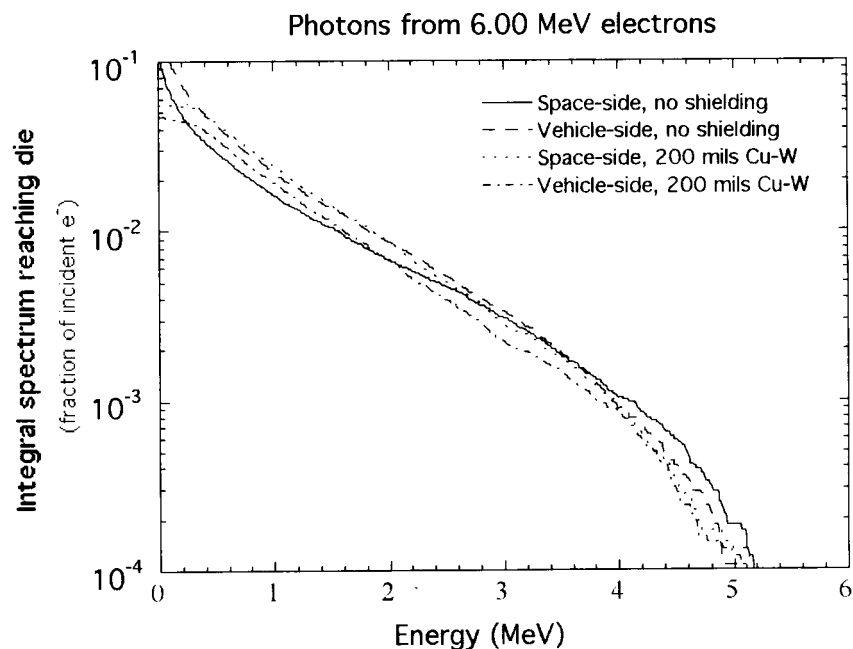


Figure 9. At 6 MeV incident electrons, the integral photon spectra for the shielded devices begins to exceed that for the unshielded at low energies.

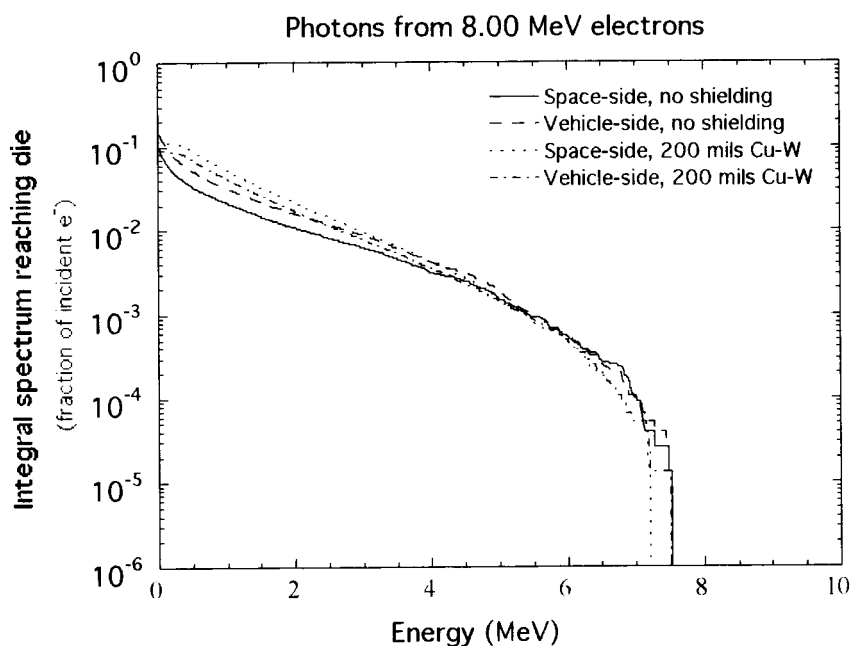


Figure 10. The low energy enhancement for the photon spectra reaching the die of the shielded parts is more pronounced for the 8 MeV incident electrons.

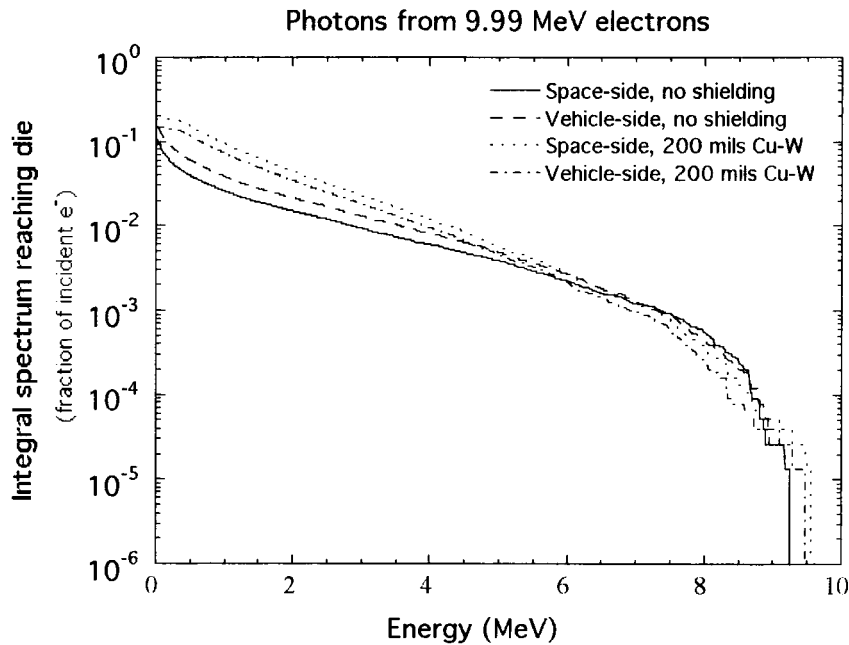


Figure 11. With 10 MeV incident electrons, the photon spectra for the shielded devices shows an enhancement for all energies up to 5 MeV reaching the die.

4.2 Low Energy Photons

A literature search turned up reports [e.g. refs 5-9] that low-energy photons like these could in fact deposit enhanced dose inside electronic microstructures, beyond their contribution to the bulk dose in the silicon. EGSnrc, however, is not the tool with which to study this phenomenon in device-level detail, because of the lower energy limits of its ability to simulate the full physics of interactions of radiation with matter. For electrons (and positrons) below 10 keV, or for photons below 1 keV, EGSnrc assumes that all of the particle's kinetic energy is deposited locally, with no further transport calculations or secondary particles generated. In silicon, a 10 keV electron has a range of about one micron, while the absorption length for a 1 keV photon is about 0.2 micron; thus the code has no way to handle the detailed variation of charge and energy deposit on scales smaller than a few times these lengths, which is far too coarse to simulate the layers of a microelectronic device. Thus, we can say that electrons of several MeV energy, which are present during the most intense enhancements of the Earth's outer radiation belts, will cause more photons to reach more heavily-shielded parts than less heavily-shielded ones, even though the overall dose to the bulk silicon is reduced by thicker shielding. However, further study with other simulation tools will be necessary in order to say whether these additional photons will cause sufficient dose enhancement within microelectronic structures to produce the degraded performance that we observed.

5. SUMMARY AND CONCLUSIONS

We have shown that the measured spectrum of energy during the geomagnetic storms in the fall of 1998 was much harder than would be predicted by tools that average over several solar cycles. The increase in high energy electrons during this series of storms will contribute to an increase in the low-energy spectra of photons reaching the die of the shielded parts. However, it will also contribute to a significant decrease in the integral spectra of electrons reaching those same dies relative to the die of the unshielded parts.

Ultimately we are still faced with the task of explaining the anomalous TID effect in the shielded devices. In order for the dose to have been worse, the contribution of the low-energy photons has to exceed that of the direct electrons on the unshielded device. In the shielded parts, the electrons are dramatically reduced. The transport codes we used to calculate dose are limited in how they handle the physics for very low energy photons (below 1 keV) and how they handle the physics of dose enhancement at the die level. More effort is needed to more accurately determine the actual dose from the electrons and the photons reaching the die. The data from the MPTB experiment indicates that the models may not be accurately predicting the result.

6. REFERENCES

1. S. H. Crain, J. E. Mazur, R. B. Katz, R. Koga, M. D. Looper, and K. R. Lorentzen, "Analog and digital single event effects experiments in space," *IEEE Trans. On Nucl. Sci.*, vol. 48, no. 6, pp. 1841-1848, Dec. 2001.
2. T. Ma and P. Dressendorfer, "Ionizing radiation effects in MOS devices and circuits," Wiley, New York, 1989.
3. Vampola, A. L., Measuring energetic electrons-what works and what doesn't, Measurement Techniques in Space Plasmas: Particles, R. F. Pfaff, J. E. Borovsky, & D. T. Young, eds., Geophys. Monograph 102, American Geophysical Union, 339, 1998.
4. J. F. Fennell, H. C. Koons, and J. B. Blake, "An internal charging environmental specification for geosynchronous and HEO/Molniya satellites," Aerospace Report no. TR-99(8570)-12, 1999.
5. J. C. Garth, E. A. Burke, and S. Woolf, "The role of scattered radiation in the dosimetry of small device structures," *IEEE Trans. On Nucl. Sci.*, vol. 27, no. 6, pp. 1459-1464, Dec. 1980.
6. D. Brown, "Photoelectron effects on the dose deposited in MOS devices by low energy X-ray sources," *IEEE Trans. On Nucl. Sci.*, vol. 27, no. 6, pp. 1465-1468, Dec. 1980.
7. D. M. Long, D. G. Millward, and J. Wallace, "Dose enhancement effects in semiconductor devices," *IEEE Trans. On Nucl. Sci.*, vol. 29, no. 6, pp. 1980-1984, Dec. 1982.
8. J. C. Garth, B. W. Murray, and R. P. Dolan, "Soft X-ray induced energy deposition in a three-layered system: Au/C/PBS," *IEEE Trans. On Nucl. Sci.*, vol. 29, no. 6, pp. 1985-1991, Dec. 1982.
9. T. R. Oldham and J. M. McGarrity, "Comparison of ^{60}Co Response and 10 KeV X-ray response in MOS capacitors," *IEEE Trans. On Nucl. Sci.*, vol. 30, no. 6, pp. 4377-4381, Dec. 1983.

REPORT DOCUMENTATION PAGE			Form Approved OMB No. 0704-0188	
Public reporting burden for this collection of information is estimated to average 1 hour per response, including the time for reviewing instructions, searching existing data sources, gathering and maintaining the data needed, and completing and reviewing the collection of information. Send comments regarding this burden estimate or any other aspect of this collection of information, including suggestions for reducing this burden, to Washington Headquarters Services, Directorate for Information Operation and Reports, 1215 Jefferson Davis Highway, Suite 1204, Arlington, VA 22202-4302, and to the Office of Management and Budget, Paperwork Reduction Project (0704-0188), Washington, DC 20503				
1. AGENCY USE ONLY (Leave Blank)		2. REPORT DATE August 2003		3. REPORT TYPE AND DATES COVERED Contractor Report
4. TITLE AND SUBTITLE TID Effects of High-Z Material Spot Shields on FPGA Using MPTB Data			5. FUNDING NUMBERS H-32489D	
6. AUTHORS S.H. Crain, J.E. Mazur, and M.D. Looper				
7. PERFORMING ORGANIZATION NAME(S) AND ADDRESS(ES) The Aerospace Corporation El Segundo, CA 90245-4691			8. PERFORMING ORGANIZATION REPORT NUMBER M-1085	
9. SPONSORING/MONITORING AGENCY NAME(S) AND ADDRESS(ES) NASA's Space Environments and Effects (SEE) Program George C. Marshall Space Flight Center Marshall Space Flight Center, AL 35812			10. SPONSORING/MONITORING AGENCY REPORT NUMBER NASA/CR-2003-212638	
11. SUPPLEMENTARY NOTES Prepared for NASA's Space Environments and Effects (SEE) Program Technical Monitor: Donna Hardage				
12a. DISTRIBUTION/AVAILABILITY STATEMENT Unclassified-Unlimited Subject Category 93 Standard Distribution Availability: NASA CASI (301) 621-0390			12b. DISTRIBUTION CODE	
13. ABSTRACT (Maximum 200 words) An experiment on the Microelectronics and Photonics Test Bed (MPTB) was testing field programmable gate arrays using spot shields to extend the life of some of the devices being tested. It was expected that the unshielded parts would fail from a total ionizing dose (TID) and yet the opposite occurred. The data show that the devices failing from the TID effects are those with the spot shields attached. This effort is to determine the mechanism by which the environment is interacting with the high-Z material to enhance the TID in these field programmable gate arrays.				
14. SUBJECT TERMS radiation, electrons, photons, FPGA, devices under test, spot shields, total ionizing dose, degradation			15. NUMBER OF PAGES 20	
			16. PRICE CODE	
17. SECURITY CLASSIFICATION OF REPORT Unclassified	18. SECURITY CLASSIFICATION OF THIS PAGE Unclassified	19. SECURITY CLASSIFICATION OF ABSTRACT Unclassified	20. LIMITATION OF ABSTRACT Unlimited	

National Aeronautics and
Space Administration

AD33

George C. Marshall Space Flight Center

Marshall Space Flight Center, Alabama

35812
